Taming Random Lasers through Active Spatial Control of the Pump

N. Bachelard,[1] J. Andreasen,[2] S. Gigan,[1] and P. Sebbah[1,*]

[1]*Institut Langevin, ESPCI ParisTech CNRS UMR7587, 1, rue Jussieu, 75238 Paris Cedex 05, France*
[2]*College of Optical Sciences, University of Arizona, Tucson, Arizona 85721, USA*
(Received 20 February 2012; published 20 July 2012)

Active control of the spatial pump profile is proposed to exercise control over random laser emission. We demonstrate numerically the selection of any desired lasing mode from the emission spectrum. An iterative optimization method is employed, first in the regime of strong scattering where modes are spatially localized and can be easily selected using local pumping. Remarkably, this method works efficiently even in the weakly scattering regime, where strong spatial overlap of the modes precludes spatial selectivity. A complex optimized pump profile is found, which selects the desired lasing mode at the expense of others, thus demonstrating the potential of pump shaping for robust and controllable single mode operation of a random laser.

Multiple scattering of light in random media can be actively manipulated through spatial shaping of the incident wave front [1]. This technique has allowed advances in focusing [2–4], and imaging [5,6], paving the road to actual control of light transport in strongly scattering media [7–9]. Introducing gain in disordered media allows amplification of multiply scattered light, leading to the observation of random lasing [10]. The broad range of systems where it has been studied [11] and the fundamental questions it has raised [12,13] have captivated the community for this last decade. Prospects of random lasing are, however, strongly hindered by the absence of emission control: random lasers are highly multimode with unpredictable lasing frequencies and polydirectional output. Manipulation of the underlying random structure [14–23] and recent work constraining the range of lasing frequencies [24,25] have resulted in significant progress toward possible control. However, the ability to choose a specific frequency in generic random lasing systems has not yet been achieved. The spatial profile of the pump is an interesting degree of freedom readily available in random lasers (e.g., [26,27]). In a regime of very strong scattering where the modes of the random system are spatially localized [28], local pumping allows selection of spatially nonoverlapping modes [29,30]. In weaker scattering media however (e.g., [31–33]), several hurdles appear toward achieving fine control. Selecting modes is complicated by a narrow distribution of lasing thresholds [34,35] and spatial mode overlap. Increased pumping required in these lossy systems begins to alter the random laser itself. Moreover, modifying the shape of the pump introduces changes to both the spatial and spectral properties of lasing modes [33,36–38]. Such difficulties are typically absent in more conventional lasers, which have employed pump shaping, both electrically [39–42] and optically [43], to select favorable lasing modes. The question is, can shaping of the incident pump field achieve taming of random lasers?

In this Letter, we exercise control over the distribution of lasing thresholds via the pump geometry to choose the random laser emission frequency. The fluctuation of lasing thresholds from mode to mode was recently found to increase when pumping a smaller spatial region [44]. Here, we demonstrate numerically that the threshold of any single lasing mode for the structures investigated can be significantly separated from its neighbors if the spatial profile of the pump is correctly chosen. An iterative approach is proposed, inspired by spatial shaping methods employed for coherent light control [1] in complex media. The optimization algorithm is based on a simple minimization criterion and can be easily implemented in experiments. We first show that the algorithm simply converges to the expected localized pump profile in the localization regime. In the weakly scattering regime, we show that mode selection is also possible despite the strong mode overlap and allows for effective monomode laser action. Strikingly, we find that the evolution of the pump profile during the optimization process alters the random laser in an advantageous way, so as to achieve the desired control.

A one dimensional random laser is represented by a stack of 161 dielectric layers (optical index n_1) separated by air gaps ($n_0 = 1.0$) (see Fig. 1). Randomness is introduced in the thickness of each layer $d_{0,1} = \langle d_{0,1}\rangle(1 + \eta\zeta)$, where $\langle d_{0,1}\rangle$ is the average thickness, $0 < \eta < 1$ the degree of randomness, and $\zeta \in [-1; 1]$ is a uniformly distributed random number. The position along the system is $x \in [0; L]$, where L is the total length. In the following, $\langle d_1\rangle = 100$ nm for the dielectric layers and $\langle d_0\rangle = 200$ nm for air, giving a total average length $\langle L\rangle = 48.1$ μm. The degree of randomness is set to $\eta = 0.9$.

We choose the dielectric material as host to the gain medium described by a frequency dependent susceptibility [38]
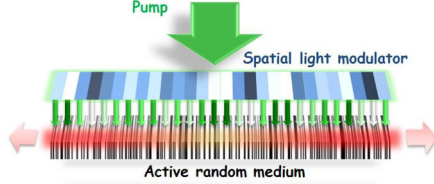
FIG. 1 (color online). Principle of active control of a 1D random laser. The black slabs represent the dielectric material which is also the gain medium. Optical pumping (small arrows) is transverse to the structure and amplitude modulated. This spatial modulation may be provided in a real experiment by a spatial light modulator. Lasing (large arrows) occurs along the structure and will depend on the pump profile.

$$\chi_g(k) = \frac{A_e N_{\text{pump}}}{k_a^2 - k^2 - ik\Delta k_a}, \tag{1}$$

where A_e is a material-dependent constant, N_{pump} is the density of excited atoms when the system is uniformly pumped, k_a is the atomic transition and Δk_a is the spectral linewidth of the atomic resonance. As a result, the refractive index of the dielectric becomes complex and frequency dependent, $n_1 \rightarrow \tilde{n}_1(k) = \sqrt{n_1^2 + \chi_g(k)}$. In the following, the transition frequency is $k_a = 10.25~\mu\text{m}^{-1}$ (typical of a solution of Rhodamine 590) and the spectral linewidth $\Delta k_a = 0.25~\mu\text{m}^{-1}$ (598–628 nm). The gain is assumed to be linear in the sense that it does not depend on the electrical field intensity, an assumption that is only valid at or below threshold. We use the transfer matrix method [38,45] to find the lasing frequency, the threshold and the spatial distribution of the lasing modes.

When partial pumping is employed, the density of excited atoms due to the pumping process is modulated according to the function f_E called the pump profile as sketched in Fig. 1. It can be written $f_E(x) \times N_{\text{pump}}$, where x is the position of the layer. The function $f_E(x)$ fulfills the constraint $0 \leq f_E(x) \leq 1$ to mimic, for instance, the amplitude modulation of the pump beam by a spatial light modulator. This pump profile changes the gain provided by each dielectric layer, giving possible control over the lasing modes of the random laser. Here, we aim at selecting a particular lasing mode by optimizing the pump profile. Experimentally, a lasing mode i will be selectively excited if its threshold, N_i, is sufficiently low and significantly lower than that of all other modes. Hence, we introduce the rejection rate, $RR_i = \min_{j \neq i}(N_j)/N_i$, which compares the threshold of mode i with that of the mode with the lowest threshold, $\min_{j \neq i}(N_j)$. Selection of mode i is achieved when $RR_i > 1$ provided its threshold, N_i remains reasonably low. We therefore minimize $1/RR_i + \alpha N_i$, with α properly chosen to balance each term [46], and apply iteratively the following algorithm. A new pump profile $f_E(x)$ results in new lasing modes and new values of RR_i and N_i. We apply the projected gradient method to $f_E(x) \rightarrow 1/RR_i + \alpha N_i$. At each iteration, the gradient of

$1/RR_i + \alpha N_i$ is computed. Then, $f_E(x)$ is tuned within $[0, 1]$ in the direction where the projected gradient of $1/RR_i + \alpha N_i$ is minimal. Convergence is assumed if its relative variation is less than 10^{-4}.

Depending on the value of the index contrast $\Delta n = n_1 - n_0$, the random laser is studied either in the strongly scattering regime, where light is confined well within the random system, or in the weakly scattering regime, where modes are extended. For an index contrast $\Delta n = 0.60$, we find a localization length $\xi \approx 1.7~\mu\text{m} \ll L$ over the spectral range $10.0~\mu\text{m}^{-1} < k < 10.5~\mu\text{m}^{-1}$. The system is therefore in the localized regime and lasing modes are spatially confined within the system. Mode selection is straightforward in this case using local pumping [29,30], given the locations of quasimodes of the passive system. The localized case serves here as a test case for our iterative algorithm to check if modes can be selected without any prior knowledge of their spatial location.

The pump profile is first initialized with a uniform profile, which is the natural pumping scheme for broad area gain lasers. The threshold and optical frequency of the lasing modes are thus computed with the profile, $f_E(x) = 1$. Ten lasing modes are found in the spectral window of interest, which are positioned in the frequency-threshold plane as crosses in Fig. 2(a). Four lasing modes with reasonably low thresholds and partial spatial overlap are chosen for demonstration. Their spatial profiles are shown in Fig. 2(b), together with the profile of a high threshold lasing mode at $k = 10.4~\mu\text{m}^{-1}$, associated with a lossy mode confined on the left end of the sample.

We then consider Mode$_2$ ($k = 10.22~\mu\text{m}^{-1}$). Its rejection rate for uniform pumping is $RR_2 = 0.45 < 1$, meaning it would not lase first at threshold. We now apply the iterative process to select this lasing mode ($\alpha = 10$ [46]). Its rejection rate increases rapidly as shown in Fig. 3(a). It is larger than unity after 10 iterations and converges to $RR_2 = 5.4$ after 57 iterations. The relative increase of its threshold is less than 50%. In contrast, all other modes see their threshold increased by at least an order of magnitude. This is illustrated in Fig. 2 which shows the evolution of the spectrum in the frequency-threshold plane. Mode$_2$ has been efficiently selected and will be the first to lase above threshold. Single mode operation will be robust even at relatively high pumping rate since RR_2 is large. The optimization algorithm has been successfully applied to all modes computed. The final rejection rates and threshold of Mode$_{i \in [1,2,3,4]}$ are given in [46].

The optimized pump profile, $f_E(x)$, obtained for Mode$_2$ is shown in Fig. 2(d) (see also movie in [46]). It is similar to the lasing mode profile, $g_2(x)$ [Fig. 2(c)]. The degree of similarity is measured by the spatial correlation $C_{f2} = \langle (f_E - \langle f_E \rangle)(g_2 - \langle g_2 \rangle) \rangle$, where f_E and g_2 have been normalized by their variance, and is close here to unity, $C_{f2} = 0.82$. The solution reached by the algorithm is therefore consistent with the predicted efficiency of a local
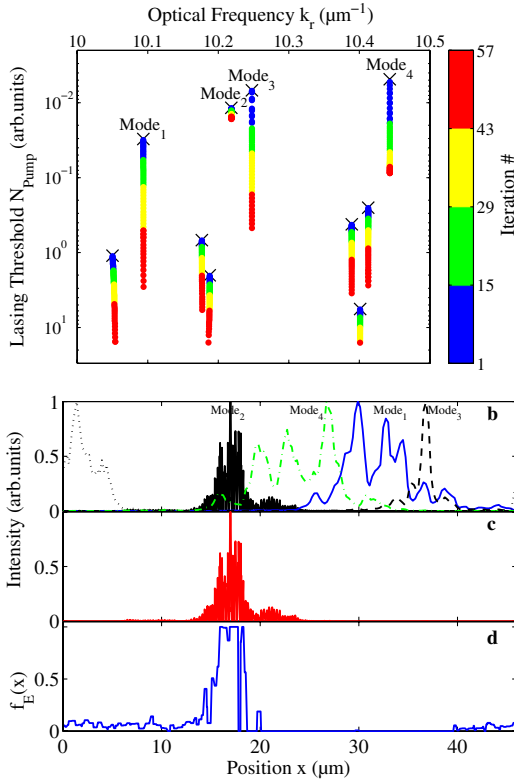
FIG. 2 (color online). Localized random laser case. (a) Frequency vs threshold of the lasing modes at successive iterations, when the optimization routine is applied to select $Mode_2$. Crosses represent initial positions for uniform pumping. (b) Spatial profile of five localized lasing modes. The mode profile on the left edge corresponds to the leaky mode with the highest threshold at $k = 10.4 \ \mu m^{-1}$. (c) Spatial profile of $Mode_2$ after optimization. (d) Resulting optimized spatial pump profile.

pumping in the localized regime, even in the presence of moderate overlap [29,30]. Also note the change of pump profile barely affects the frequency [Fig. 2(a)] and spatial profile [Fig. 2(c)] of the lasing modes, as expected in the localized regime [13].

For more detail concerning the operation of the algorithm, we examine the evolution of the evolution of the correlations $C_{fi \in [1,2,3,4]}$ of the pump profile with $Mode_{i \in [1,2,3,4]}$. As the optimization routine is applied, C_{f2} consistently increases, while correlations $C_{fi \in [1,3,4]}$ of the other modes are progressively minimized, as shown in Fig. 3(c), resulting in increased thresholds for these modes. The crosses in Fig. 3(c) indicate the mode with lowest threshold, $\min_{j \neq 2}(N_j)$, entering the calculation of RR_2 at a given iteration. After working alternatively on $Mode_3$ and $Mode_4$, the algorithm works exclusively on the rejection of $Mode_4$. This mode has the largest overlap with $Mode_2$; a fine tuning of the pump profile is therefore required to increase its threshold without greatly increasing the threshold of $Mode_2$.
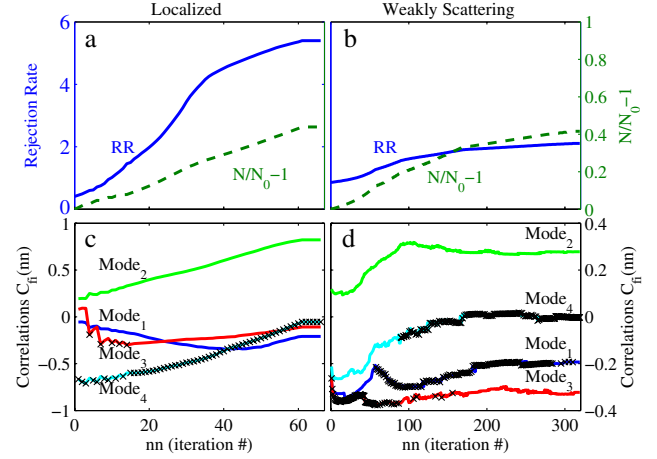

FIG. 3 (color online). (a),(c) Localized case, (b),(d) weakly scattering case. (a),(b) Rejection rate, RR_2, and threshold N_2 for selected mode. (c),(d) Spatial correlations functions, C_{fi}, between pump profile and $Mode_i$. Crosses indicate the mode with lowest threshold entering the calculation of RR_2.

We turn now to the more difficult case of a weakly scattering random laser. For an index contrast of $\Delta n = 0.05$, the localization length is $\xi \approx 200 \ \mu m \gg L$ over the frequency range $10.0 \ \mu m^{-1} < k < 10.5 \ \mu m^{-1}$. Lasing modes are spatially extended over the whole system, as illustrated in Fig. 4(a).

Figures 3(b), 3(d), and 4 present the results for the selection of $Mode_2$ ($k = 10.23 \ \mu m^{-1}$ and $RR_{20} = 0.86$) ($\alpha = 0.3$ [46]). The algorithm converges after 320 iterations with a final rejection rate $RR_2 = 2.47$. Although more modest than in the localized case, this increase is significant enough to envision monomode operation of the random laser at that selected frequency. Higher-threshold mode suppression, which occurs through gain saturation and mode interaction [47,48], was verified for the optimized pump profile by taking these effects into account through a different numerical model [30]. Similar results are obtained for all other modes tested [46]. Figure 4(a) shows the relative impact of the iterative process on $Mode_2$ and on the other modes. As the thresholds increase, lasing modes experience spectral shifts as well as spatial deformation [Fig. 4(c)], in contrast to the localized case. This is a direct consequence of the strong level of pumping required and to the non-uniformity of the gain profile. Figure 4(d) shows the optimized pump profile (also, see movie in [46]). Such a profile is unpredictable. A small correlation $C_{f2} = 0.28$ [Fig. 3(d) and [46]] is found only when comparing the stationary component of the mode [Fig. 4(c)] [38] and the pump profile. The strength of our adaptive approach is revealed in this case where mode overlap is significant, threshold distribution is fairly narrow and nonlinear effects strongly impact the modes. The subtlety of the optimization process, which is successfully demonstrated for all modes, is exemplified in Fig. 3(d) where the ceaseless switching between modes
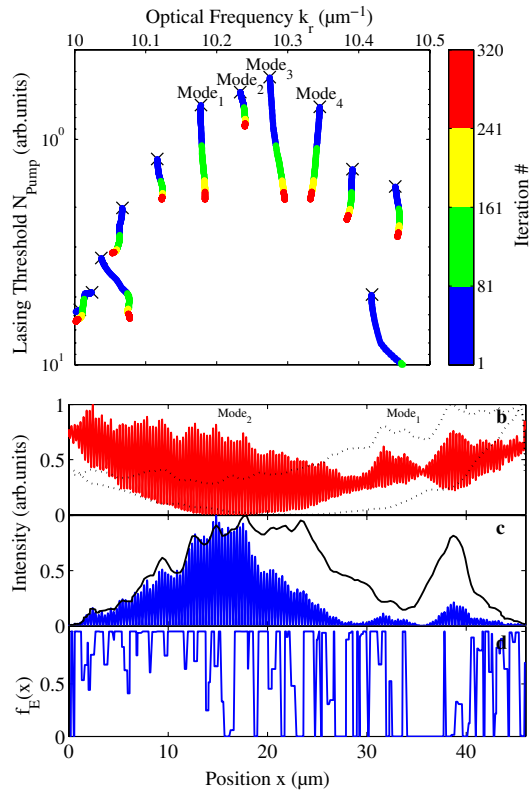
FIG. 4 (color online). Weakly scattering random laser case.
(a) Frequency vs threshold of the lasing modes at successive
iterations, when the optimization routine is applied to select
Mode$_2$. Crosses represent initial positions for uniform pumping.
(b) Spatial profile of Mode$_1$ (envelope) and Mode$_2$ (full).
(c) Stationary component of Mode$_2$ before (envelope) and after
optimization (full). (d) Resulting optimized spatial pump profile.

Mode$_{i \in [1,3,4]}$ (crosses) forces reduced correlation and even
anticorrelation between the rejected modes and the pump
profile.

We have intentionally chosen a small index contrast
to test the extreme case of a weakly scattering system
($\xi \gg L$) but mode selection worked successfully for inter-
mediate regime of scattering as well. We also chose
intentionally to compare only two modes at each iteration
because such a weakly constrained optimization criterion
ensures rapid convergence and is relatively easy to imple-
ment in a real experiment. The role of initial conditions
(initial profile) and the stability of the solutions have been
tested. If the solution is in general robust in the localized
regime, local minima are most often reached in the weakly
scattering regime. The choice of initial conditions is ex-
pected to be more critical in an experiment. We tested a
global optimization based on the Ant algorithm [49] on a
small subset of variables, which yielded promising results.
A full global optimization, however, is numerically out of
reach at the moment. Though the systems studied here
with a narrow range of emission frequencies have
experimental analogs [24,25], typical weakly scattering

random lasers yield a huge number of closely packed
lasing modes. In such cases, an efficient global optimiza-
tion may be necessary, and therefore, is under develop-
ment. Finally, it is worthwhile pointing out that the
optimization problem posed here is different from [7] since
the iterative process is highly nonlinear: the medium itself
is modified at each iteration by the new computed pump
profile. Surprisingly, the alterations to the random laser
induced by the pump profile are used to the advantage of
the optimization routine, and do not hinder the goal of
mode selection.

In summary, we have demonstrated numerically that
control of the lasing emission frequency is possible in a
random laser. Active control of the pump profile is pro-
posed to select any lasing mode in the emission spectrum
by significantly increasing the threshold of others. The
method has been successfully tested in the regime of strong
scattering where modes are spatially localized and can be
easily selected using local pumping. In the weakly scatter-
ing regime where strong spatial mode overlap precludes
any straightforward spatial selectivity, the algorithm re-
markably converges to a complex optimized pump profile
which selects the desired lasing mode. The proposed algo-
rithm is straightforward to implement in practice. It also
provides an optimized solution which limits the pump flux
on the sample and, for instance, reduces optical damage.
These results open further the way to active control of the
lasing properties of random systems by shaping of the
pump profile. On the basis of our results, we believe output
directionality may also be achieved. For example, local
pumping has been shown to yield unidirectional emission
in random lasers through the selection of a new lasing
mode [50] generated by the presence of gain boundaries
[51]. Additionally, relaxing the constraint of mode
selection may allow a combination of lasing modes to
produce the desired directionality. Moreover, because par-
tial pumping modifies the spatial distributions of lasing
modes, the output is not bound by the parameters of the
passive random system. For instance, the frequency shift
observed in the weakly diffusive case could be manipulated
to tune at will the emission frequency of the laser. Realistic
1D random lasers exist [52], though extension to higher
dimensions may also be possible. Phase sensitive wave
front shaping [53] should allow selective pumping deep
inside 3D samples by adapting the pump intensity distri-
bution inside the medium. Furthermore, we believe
this method can be extended to the domain of optically
pumped broad gain area lasers, such as high-power broad-
area semiconductor lasers where it can be an alternative to
the issue of filamentation in order to optimize their bright-
ness [54].

*patrick.sebbah@espci.fr

[1] I. M. Vellekoop and A. P. Mosk, Opt. Lett. **32,** 2309 (2007).

[2] I. M. Vellekoop, A. Lagendijk, and A. P. Mosk, Nature Photon. **4,** 320 (2010).

[3] T. Čižmár, M. Mazilu, and K. Dholakia, Nature Photon. **4,** 388 (2010).

[4] E. Martin-Badosa, Nature Photon. **4,** 349 (2010).

[5] S. M. Popoff, G. Lerosey, M. Fink, A. C. Boccara, and S. Gigan, Nature Commun. **1,** 81 (2010).

[6] A. J. Thompson, C. Paterson, M. A. A. Neil, C. Dunsby, and P. M. W. French, Opt. Lett. **36,** 1707 (2011).

[7] I. M. Vellekoop and A. P. Mosk, Phys. Rev. Lett. **101,** 120601 (2008).

[8] J. Pendry, Physics **1,** 20 (2008).

[9] S. M. Popoff, G. Lerosey, R. Carminati, M. Fink, A. C. Boccara, and S. Gigan, Phys. Rev. Lett. **104,** 100601 (2010).

[10] H. Cao, Waves Random Media **13,** R1 (2003).

[11] D. S. Wiersma, Nature Phys. **4,** 359 (2008).

[12] O. Zaitsev and L. Deych, J. Opt. **12,** 024001 (2010).

[13] J. Andreasen *et al.*, Adv. Opt. Photon. **3,** 88 (2011).

[14] D. S. Wiersma and S. Cavalieri, Nature (London) **414,** 708 (2001).

[15] K. Lee and N. M. Lawandy, Opt. Commun. **203,** 169 (2002).

[16] X. H. Wu, A. Yamilov, H. Noh, H. Cao, E. W. Seelig, and R. P. H. Chang, J. Opt. Soc. Am. B **21,** 159 (2004).

[17] J. Ripoll, C. M. Soukoulis, and E. N. Economou, J. Opt. Soc. Am. B **21,** 141 (2004).

[18] S. Gottardo, S. Cavalieri, O. Yaroshchuk, and D. S. Wiersma, Phys. Rev. Lett. **93,** 263901 (2004).

[19] C. Vanneste and P. Sebbah, Phys. Rev. E **71,** 026612 (2005).

[20] T. Savels, A. P. Mosk, and A. Lagendijk, Phys. Rev. Lett. **98,** 103601 (2007).

[21] S. Gottardo, R. Sapienza, P. D. García, A. Blanco, D. S. Wiersma, and C. López, Nature Photon. **2,** 429 (2008).

[22] H. Fujiwara, Y. Hamabata, and K. Sasaki, Opt. Express **17,** 3970 (2009).

[23] H. K. Liang, S. F. Yu, and H. Y. Yang, Appl. Phys. Lett. **97,** 241107 (2010).

[24] R. Bardoux, A. Kaneta, M. Funato, K. Okamoto, Y. Kawakami, A. Kikuchi, and K. Kishino, Opt. Express **19,** 9262 (2011).

[25] R. G. S. El-Dardiry and A. Lagendijk, Appl. Phys. Lett. **98,** 161106 (2011).

[26] M. Leonetti, C. Conti, and C. Lopez, Nature Photon. **5,** 615 (2011).

[27] H. Kalt, Nature Photon. **5,** 573 (2011).

[28] P. W. Anderson, Phys. Rev. **109,** 1492 (1958).

[29] C. Vanneste and P. Sebbah, Phys. Rev. Lett. **87,** 183903 (2001).

[30] P. Sebbah and C. Vanneste, Phys. Rev. B **66,** 144202 (2002).

[31] S. V. Frolov, Z. V. Vardeny, K. Yoshino, A. Zakhidov, and R. H. Baughman, Phys. Rev. B **59,** R5284 (1999).

[32] Y. Ling, H. Cao, A. L. Burin, M. A. Ratner, X. Liu, and R. P. H. Chang, Phys. Rev. A **64,** 063808 (2001).

[33] X. Wu, W. Fang, A. Yamilov, A. A. Chabanov, A. A. Asatryan, L. C. Botten, and H. Cao, Phys. Rev. A **74,** 053812 (2006).

[34] M. Patra, Phys. Rev. E **67,** 016603 (2003).

[35] V. M. Apalkov and M. E. Raikh, Phys. Rev. B **71,** 054203 (2005).

[36] R. C. Polson and Z. V. Vardeny, Phys. Rev. B **71,** 045205 (2005).

[37] X. Wu, J. Andreasen, H. Cao, and A. Yamilov, J. Opt. Soc. Am. B **24,** A26 (2007).

[38] J. Andreasen, C. Vanneste, L. Ge, and H. Cao, Phys. Rev. A **81,** 043818 (2010).

[39] C. Gmachl, F. Capasso, E. E. Narimanov, J. U. Nöckel, A. D. Stone, J. Faist, D. L. Sivco, and A. Y. Cho, Science **280,** 1556 (1998).

[40] M. Hentschel and T. Y. Kwon, Opt. Lett. **34,** 163 (2009).

[41] S. Shinohara, T. Harayama, T. Fukushima, M. Hentschel, T. Sasaki, and E. E. Narimanov, Phys. Rev. Lett. **104,** 163902 (2010).

[42] A. D. Stone, Nature (London) **465,** 696 (2010).

[43] D. Naidoo, T. Godin, M. Fromager, E. Cagniot, N. Passilly, A. Forbes, and K. Aït-Ameur, Opt. Commun. **284,** 5475 (2011).

[44] J. Andreasen and H. Cao, Opt. Express **19,** 3418 (2011).

[45] X. Jiang and C. M. Soukoulis, Phys. Rev. E **65,** 025601 (2002).

[46] See Supplemental Material at http://link.aps.org/supplemental/10.1103/PhysRevLett.109.033903 for a table of values and movies.

[47] J. Andreasen, P. Sebbah, and C. Vanneste, J. Opt. Soc. Am. B **28,** 2947 (2011).

[48] H. E. Türeci, L. Ge, S. Rotter, and A. D. Stone, Science **320,** 643 (2008).

[49] M. Schlüter and M. Gerdts, J. Global Optim. **47,** 293 (2010).

[50] J. Andreasen and H. Cao, Opt. Lett. **34,** 3586 (2009).

[51] L. Ge, Y. D. Chong, S. Rotter, H. E. Türeci, and A. D. Stone, Phys. Rev. A **84,** 023820 (2011).

[52] See, e.g., V. Milner and A. Z. Genack, Phys. Rev. Lett. **94,** 073901 (2005).

[53] I. M. Vellekoop, E. G. van Putten, A. Lagendijk, and A. P. Mosk, Opt. Express **16,** 67 (2008).

[54] J. Ohtsubo, *Semiconductor Lasers: Stability, Instability and Chaos*, Springer Series in Optical Sciences Vol. 111 (Springer, New York, 2007).